

# SANDIA REPORT

SAND97-0170 • UC-506

Unlimited Release

Printed January 1997

## A Tool to Detect External Cracks from Within a Metal Tube

Thurlow W. H. Caffey

Prepared by  
Sandia National Laboratories  
Albuquerque, New Mexico 87185 and Livermore, California 94550  
for the United States Department of Energy  
under Contract DE-AC04-94AL85000

Approved for public release; distribution is unlimited.

Issued by Sandia National Laboratories, operated for the United States Department of Energy by Sandia Corporation.

**NOTICE:** This report was prepared as an account of work sponsored by an agency of the United States Government. Neither the United States Government nor any agency thereof, nor any of their employees, nor any of their contractors, subcontractors, or their employees, makes any warranty, express or implied, or assumes any legal liability or responsibility for the accuracy, completeness, or usefulness of any information, apparatus, product, or process disclosed, or represents that its use would not infringe privately owned rights. Reference herein to any specific commercial product, process, or service by trade name, trademark, manufacturer, or otherwise, does not necessarily constitute or imply its endorsement, recommendation, or favoring by the United States Government, any agency thereof or any of their contractors or subcontractors. The views and opinions expressed herein do not necessarily state or reflect those of the United States Government, any agency thereof or any of their contractors.

Printed in the United States of America. This report has been reproduced directly from the best available copy.

Available to DOE and DOE contractors from  
Office of Scientific and Technical Information  
PO Box 62  
Oak Ridge, TN 37831

Prices available from (615) 576-8401, FTS 626-8401

Available to the public from  
National Technical Information Service  
US Department of Commerce  
5285 Port Royal Rd  
Springfield, VA 22161

NTIS price codes  
Printed copy: A08  
Microfiche copy: A01

Errata, SAND97-0170

The following was omitted, in printing, from the reverse side of the title page:

### **Acknowledgment**

I wish to thank James R. Wait, Professor Emeritus of the University of Arizona, and David A. Hill, of the National Institute of Science and Technology at Boulder, Colorado, for discussions of their paper which was the basis for the computation of the electromagnetic fields. Herman A. Watts, Department 1273, provided a derivation which significantly decreased the computation time.

On page 7, replace the paragraph beginning Distance with:

Distance. Increasing the antenna separation distance is dubious for two reasons: The allowance for the scattering loss would have to be increased because of the greater scattering angle, and the increased path length in the metal would further decrease the signal because of the exponential attenuation.

SAND 97-0170  
Unlimited Release  
Printed January 1997

Distribution  
Category UC-506

## A Tool to Detect External Cracks from within a Metal Tube

Thurlow W. H. Caffey  
Geophysical Technology Department  
Sandia National Laboratories  
Albuquerque, NM 87185-0705

### **Abstract**

A tool using a continuous electromagnetic wave from a transverse magnetic-dipole source with a coaxial electric-dipole receiver is outlined for the detection of external sidewall cracks in boiler tubes. A numerical study of the distribution of the fields shows that the direct transmission from the source to the receiver is reduced from that in free space. Further, if the diameter of the receiver dipole is made sufficiently small, it should be possible to detect cracks with a scattering loss of up to -40dB in thin-walled boiler tubes.

## Contents

Preface .....	1
Introduction .....	1
The Primary Field .....	2
The Total Field within the Tube .....	4
An Example .....	4
Conclusion .....	11
References .....	11
Appendix: Electromagnetic Fields in a Cylindrical Void within a Complex Media .....	12

### Figures

1	Relative Ez-Field from an X-directed magnetic dipole at any spherical radius .....	5
2	Relative Ez-Field within a 2.2cm metal tube at $Z = 0$ .....	6
3	Relative Ez-Field within a 2.2cm metal tube at $Z = 1.1\text{cm}$ .....	8
4	Relative Ez-Field within a 2.2cm metal tube at $Z = 2.2\text{cm}$ .....	9
5	Relative Ez-Field within a 2.2cm air tube at $Z = 2.2\text{cm}$ .....	10
A1	Cross-section geometry for a cylindrical void .....	13
A2	Magnitude of the relative Ez-Field in air within a radius of 1.1cm in the XY-plane .....	16
A3	Difference between computations with azimuth as a parameter .....	17

# A Tool to Detect External Cracks from within a Metal Tube

## Preface

Historically, and even to the present day, the major cause of boiler outages is the degradation of the steam tubes by which heat is extracted from the boiler. Although there is deposition and corrosion upon the internal surfaces of the tubes, the principal cause of failure is by the development of exterior cracks. Of course, when a boiler is otherwise down for repair, the exteriors of all apparently satisfactory tubes are inspected for cracking. Unfortunately, some cracks may not be discovered because the exterior surfaces are more or less covered by combustion or corrosion products. A inspection tool that could be passed through a boiler tube, and detect an unseen sidewall crack from within, would increase the intervals between boiler outage and provide substantial cost savings.

This work was done as a six-week effort under Laboratory Directed Research & Development Project #3536.

## Introduction

The basic idea is to transmit an electric field which is parallel to the axis of the tube, and which will reflect off the exterior wall and return to an internal receiver. It is assumed that the return from a crack-anomaly will be distinguishable from that of an acceptable part of the tube wall, and that the interior of the tube is filled with air. A pulse-type system cannot be used because the small dimensions of boiler tubes, whose inner diameters are generally 10cm or less, would require such a high-frequency system that the thickness of the metal wall would completely absorb the electromagnetic field before the field could reach the exterior.

A single-frequency, continuous-wave system, in which the transmitting and receiving antennas are designed to minimize the crosstalk between them, is presented here. The crosstalk constitutes a 'self-clutter' which will set the lower bound to the signal-to-noise ratio of the system. The choice of operating frequency must fulfill these opposing criteria:

1. The frequency must be low enough that the round-trip attenuation along the two-way path in the metal will be small enough to allow a detectable returned signal level at the receiver. This attenuation constraint upon the frequency will ensure that the operating frequency is below the cutoff frequency of the cylindrical waveguide formed by the tube. In other words, the receiver will not be excited by a waveguide mode *per se*. As a practical matter, to ensure detectability, I require that the rms returned signal be at least twice as great as the rms level of the clutter.

2. The frequency must be high enough so that cracks of some specified minimum size can be detected.

These two criteria are not separable, and, to make matters worse, the fractional amount of the field incident upon an anomaly that will be returned toward the interior of the tube is not yet known. I will assume that this *scattering loss* is fixed at 1/100 (-40dB) for present purposes.

One way to examine the effect of both frequency and clutter is to compare the magnitude of the field transmitted into the tube wall, attenuated by the both path loss and scattering loss, with the magnitude of the self-clutter field. This signal-to-clutter ratio, or *SCR*, can be written as follows:

$$E_{signal,rms} = E_{transmit,rms} \left( \frac{e^{-2d/\delta}}{100} \right), \quad (1)$$

where  $d$  = wall-thickness of the tube, and  $\delta$  = the skindepth (later defined). The SCR is defined as

$$SCR(dB) = 20 \text{Log} \left( \frac{E_{signal,rms}}{E_{clutter,rms}} \right), \quad (2)$$

which becomes:

$$SCR(dB) = 20 \text{Log} \left( \frac{E_{transmit,rms}}{E_{clutter,rms}} \right) - \frac{17.37d}{\delta} - 40, \quad (3)$$

In this formula the 2<sup>nd</sup> term is the two-way path loss, the 3<sup>rd</sup> term is the scattering loss, and  $E_{transmit}$  and  $E_{clutter}$  are computed according to Wait and Hill, (1977).

The target will be considered detectable only if the SCR is 6dB or more. A discussion of the computation of the fields with application of the SCR to a metal boiler tube is given below.

## The Primary Field

Because the use of an electric field parallel to the tube axis is considered, it is desirable to have a transmitter which not only provides such a field at the interior wall of the tube, but which also has an absence of such a field elsewhere in the tube where a receiving element could be placed.

Consider a Cartesian coordinate system in which the Z-axis will later be placed along the axis of an air-filled tube. In the absence of the tube, the Z-component of the electric field provided by an infinitesimal magnetic dipole whose moment is along the X-axis is given by:

$$E_z = \frac{-j\mu\omega IdA}{4\pi} \sin\theta \sin\phi \left( \frac{jkR-1}{R^2} \right) e^{jkR}, \quad \text{V/m (4)}$$

where:

$$j = \sqrt{-1};$$

$\mu$  = permeability of free space, Henries/meter;

$\omega = 2\pi f$  = radian frequency, seconds<sup>-1</sup>;

$k = \alpha + j\beta$  = the propagation factor, meters<sup>-1</sup>;

$$\text{with } \alpha = \frac{\omega\sqrt{\epsilon_r}}{c} \cdot \sqrt{\frac{+1 + \sqrt{1+g^2}}{2}},$$

$$\beta = \frac{\omega\sqrt{\epsilon_r}}{c} \cdot \sqrt{\frac{-1 + \sqrt{1+g^2}}{2}},$$

$$g = \frac{\sigma}{\omega\epsilon_r\epsilon_0} = \text{the loss tangent};$$

$\epsilon_0$  = the dielectric constant of free space, Farads/m;

$\epsilon_r$  = the relative dielectric constant;

$\sigma$  = conductivity, Siemens/m;

$c$  = speed of electromagnetic propagation in free space, m/s;

$I$  = dipole current, peak Amperes;

$dA$  = dipole area, meter<sup>2</sup>;

and  $(R, \theta, \phi)$  are the usual spherical coordinates. This formula for  $E_z$  is not defined at the origin,  $R = 0$ , where the magnetic dipole is located. The magnitude of  $E_z$  is a maximum in the plane  $\theta = 90^\circ$  and along the direction  $\phi = \pm 90^\circ$ , and is zero whenever either  $\theta$  or  $\phi$  are either  $0^\circ$  or  $180^\circ$ . In the Cartesian coordinates,  $E_z$  is a maximum along the  $\pm Y$ -axis and is zero in the  $XZ$ -plane aside from the origin. An infinitesimal electric dipole, aligned parallel to the Z-axis and placed anywhere in the  $XZ$ -plane, aside from the origin, would be completely uncoupled from the transmitter. However, a physical dipole will always have a non-zero cylindrical radius, and its effect on self-clutter will be examined later.

If the magnitude of  $E_z$  is written-out, the terms in  $R$  may be collected into one factor, and the angular distribution of  $|E_z|$  is seen to be the same for any spherical radius greater than zero:

$$|E_z| = \frac{\mu\omega IdA}{4\pi} \left( \frac{\sqrt{(\alpha R)^2 + (1 + \beta R)^2}}{R^2} \exp(-\beta R) \right) \sin\theta |\sin\phi| \quad (5)$$

This distribution is shown in Fig. 1 in which the half-power beamwidth of each lobe is  $90^\circ$ . The bi-lobed distribution describes the primary field even when the magnetic dipole is enclosed by a cylindrical metal tube of radius ' $\rho$ ' as long as  $R \leq \rho$ .

### The Total Field within the Tube

The theory of the total field within a metal tube is described in Appendix A. The Z-component of the internal electric field is the sum of the primary field from the magnetic dipole,  $E_{PRIMARY}$ , and the field reflected from the wall,  $E_{REFLECTED}$ :

$$E_z = E_{PRIMARY} + E_{REFLECTED} \quad (6)$$

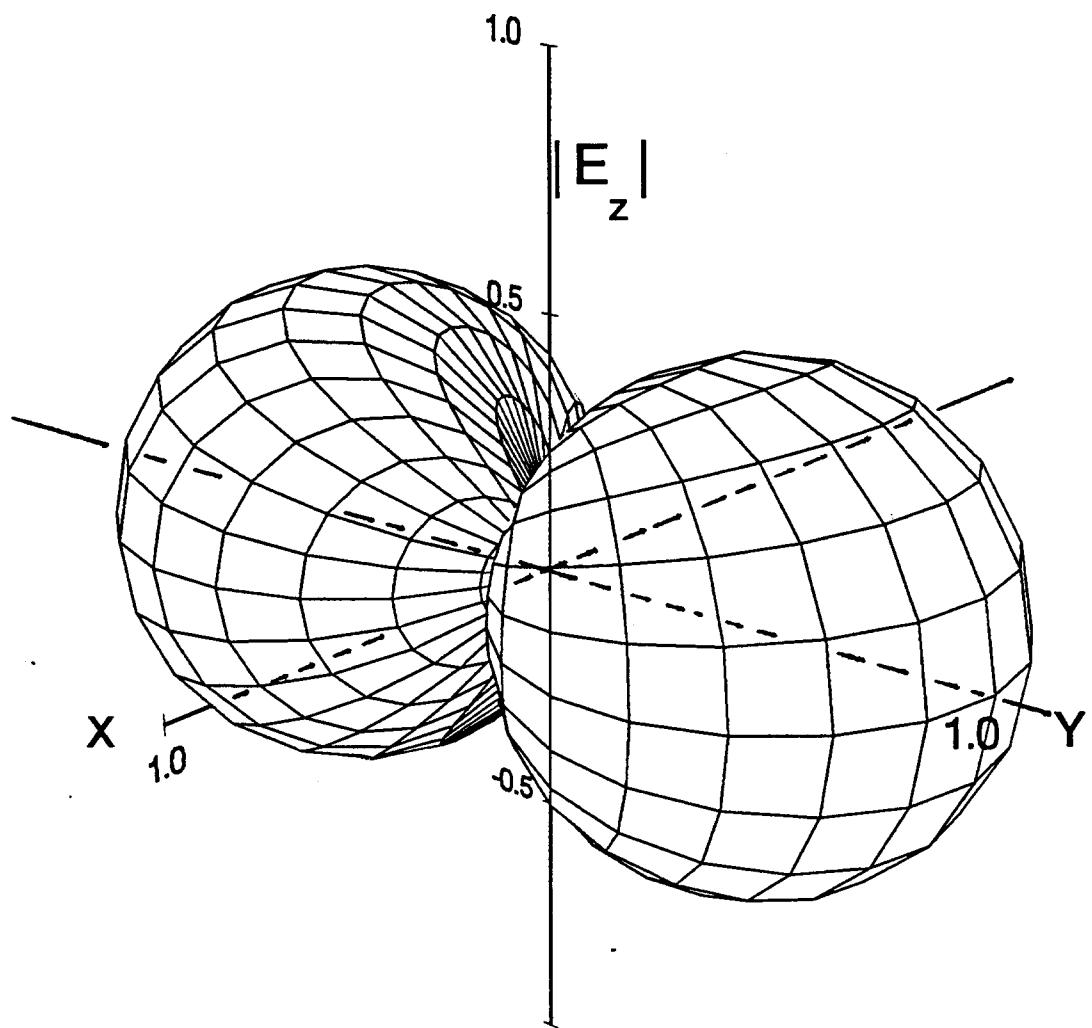
The field transmitted into the tube wall,  $E_{TRANSMIT}$ , or  $E_T$ , is equal to  $E_z$  evaluated at the interior air/tube boundary because of the continuity of the tangential components of the E-field. In a metal tube, at frequencies below the infrared, the parts of the propagation constant are equal to each other, namely  $\alpha = \beta = \sqrt{\mu\omega\sigma/2}$ , and attenuation through the wall thickness ' $d$ ' occurs as  $\exp(-d/\delta)$  where  $\delta$  is the 'skindepth' given by  $\delta = 1/\alpha$ .

### An Example

An Inconel tube with an inner diameter of 2.2cm, a wall-thickness of 0.127cm, and a conductivity of  $8.2E6$  S/m is typical of the smallest tube commonly found in boilers. The frequency of 47.88KHz will be used to make the two-way path through the wall equal to one skindepth so that the second term in Eq.(3) becomes -8.7dB. In the following figures, the fields will be presented as normalized surfaces in cylindrical coordinates in which radial distances are relative to the tube radius. The increments of normalized radius and polar angle will be 0.1 and  $10^\circ$  respectively.

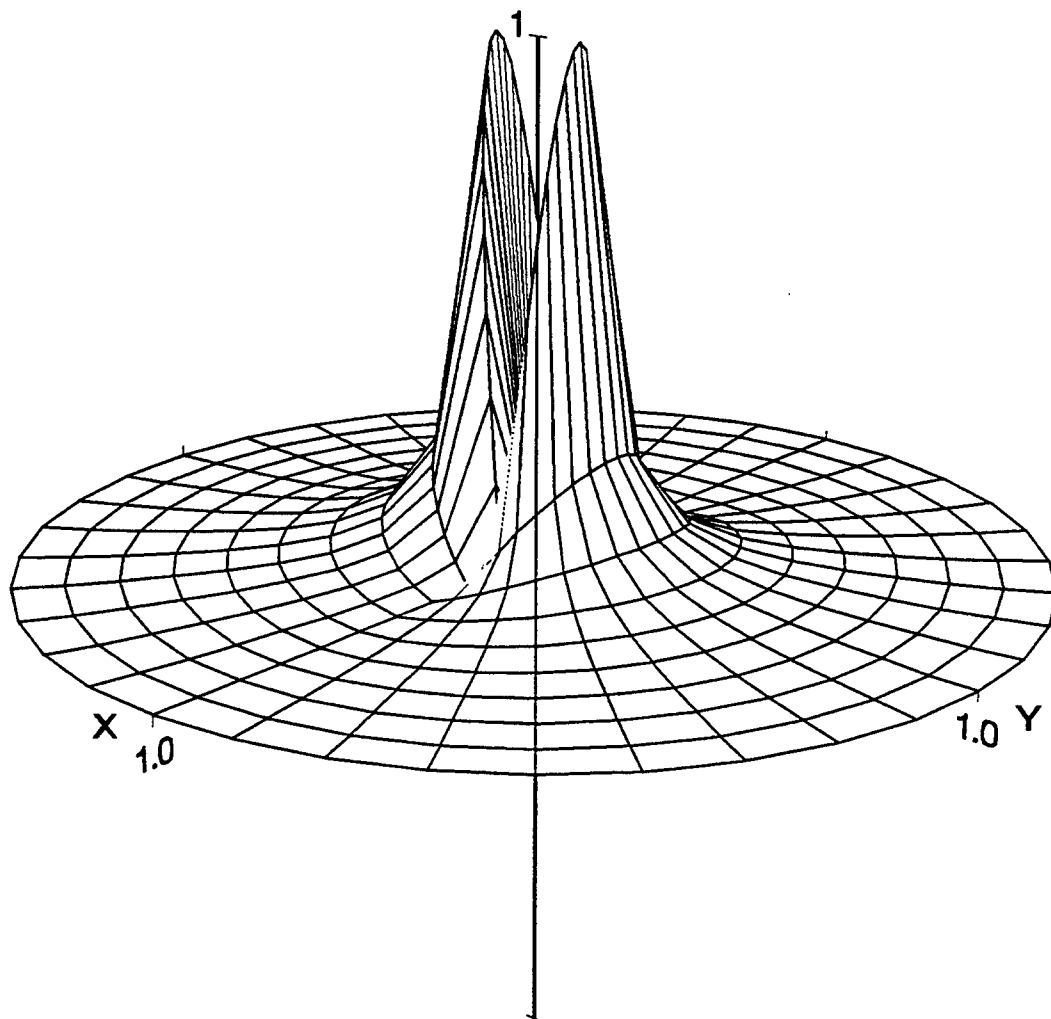
Figure 2 illustrates the relative magnitude of  $E_z$  in the  $XY$ -plane. The figure is dominated by the double-peaks near the  $Z$ -axis. These occur because the field is computed ever more closely to the magnetic dipole located at the origin (where the graph is set to zero for display purposes). When the field along the tube wall at  $\rho = 1$  is examined closely, the field is seen to vary as the cosine of the polar angle rather than as the sine-function of the primary field, Eq.(4). This effect is caused by the large loss tangent which occurs in the metal tube. A small,  $Z$ -oriented, electric dipole placed anywhere within Fig. 2 would be excited by strong  $E_z$ -fields, and provide a large self-clutter.

Figure 1  
Relative  $|E_z\text{-field}|$  from an X-directed magnetic dipole  
at any spherical radius greater than zero



hmdxez1.dcf  
hmdezf01.dat

Figure 2  
Relative Ez-field with a 2.2cm metal tube at  $Z = 0$



ctube6a.dcf  
ctube6a.dat  
ctube6a.wk1  
ctubeo.06a

Figure 3 shows the relative magnitude of  $E_Z$  in the plane where  $Z$  is one tube radius. The cosine-nature of the field along the boundary is now very apparent. The surface varies rapidly, but the  $Z$ -axis could be considered as a location for the receiving antenna.

Figure 4 shows the relative magnitude of  $E_Z$  in the plane where  $Z$  is one tube diameter. The surface appears as a folded disc, curved slightly downward at the outer edge, and with an undulation along the  $Y$ -axis which falls to zero at the center and at  $Y = \pm 1$ . The primary field alone is shown in Fig. 5, and, by comparison with Fig. 4, vividly demonstrates the rotation due to the reflecting boundary.

Suppose a small electric dipole, with a radius of one-tenth the tube radius, is placed at the origin in Fig. 4. The self-clutter field at the receiver is estimated as the mean value of the field along  $\rho = 0.1$ . Suppose further that a crack is located along the exterior tube wall in the  $XY$ -plane which is also the location of the source at  $Z = 0$ . The ratio of  $E_{TRANSMIT}$  to  $E_{CLUTTER}$ , the first term in Eq.(3) is about 43.6dB, but the SCR is -5.1dB which is below the detectability criteria. Any other  $Z$ -location of a crack will further reduce the SCR. For example, if the crack is located at  $Z =$  one tube radius, the  $E_T$  field is reduced by 3dB because of the beamwidth of the primary field, and the SCR decreases to -8.1dB.

The problem is that the reflected field does not sufficiently reduce the primary field at the location of the receiving antenna. For example, using Figures 4 and 5, the ratio of the self-clutter field with the tube present, to the field with the tube absent, is only -12.6 dB. There are three changes that can be made:

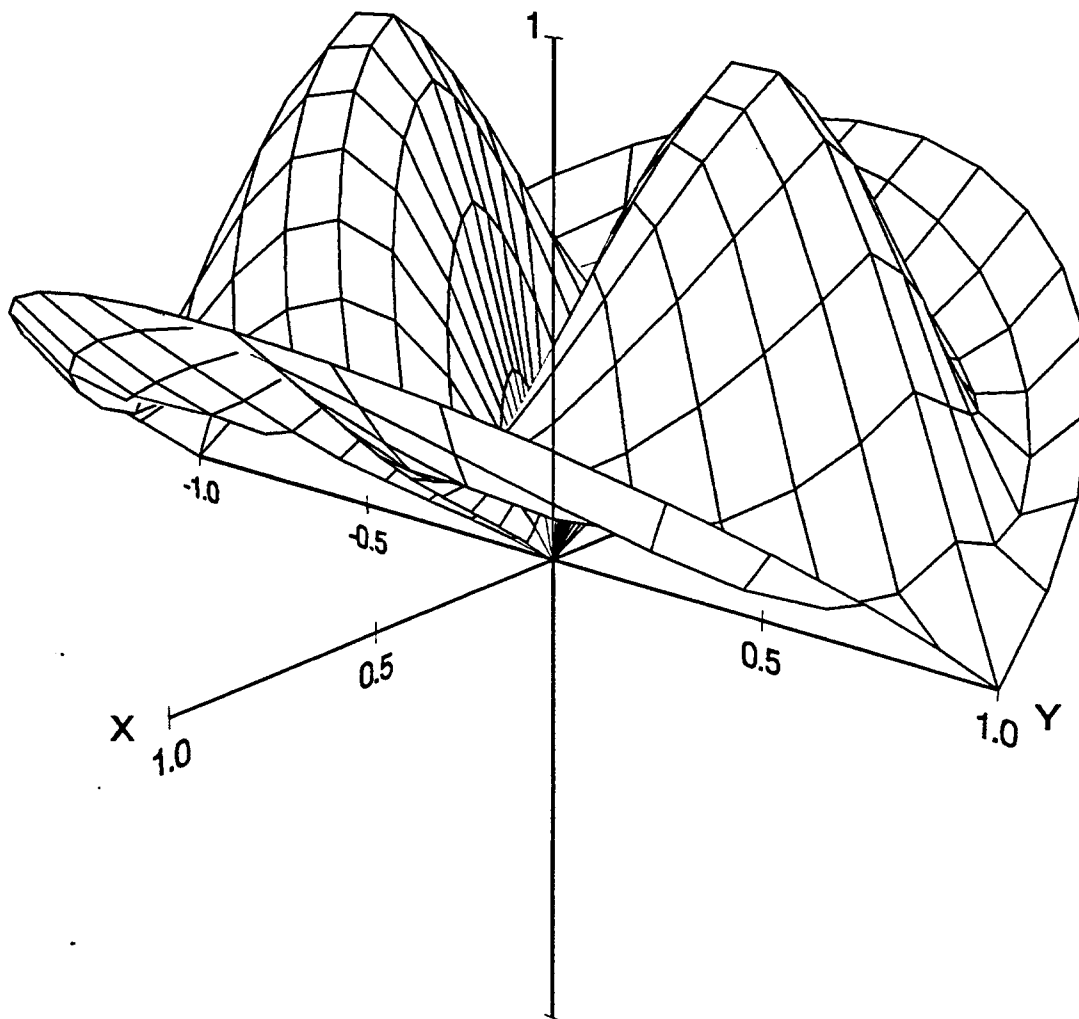
- Increase the antenna separation distance
- Change the operating frequency
- Reduce the diameter of the electric dipole.

Distance. Increasing the antenna separation distance is dubious for two reasons: The allowance for the scattering loss would have to be increased because of the increased path length in the metal.

Frequency. If the frequency is increased by a factor of 4, the  $E_T$  field increases by 7.3dB, but the skin depth is halved and the path loss increases by 8.7dB. The self-clutter increases by about 5.4dB, and the net result is that the SCR decreases from -5.1dB to -11.9dB. If the frequency is decreased by a factor of 4, the  $E_T$  field decreases by 8.4dB, but the skin depth is doubled and the path loss decreases by 4.3dB. The self-clutter decreases by 5.5dB, and the net result is that the SCR decreases from -5.1dB to -3.6dB. By how much can the frequency be decreased in an effort to raise the SCR to 6dB? This question cannot be answered without a model library of cracks and their scattering loss, but the scattering loss will eventually increase with decreasing frequency as the maximum dimension of the crack becomes a smaller fraction of the wavelength in the metal.

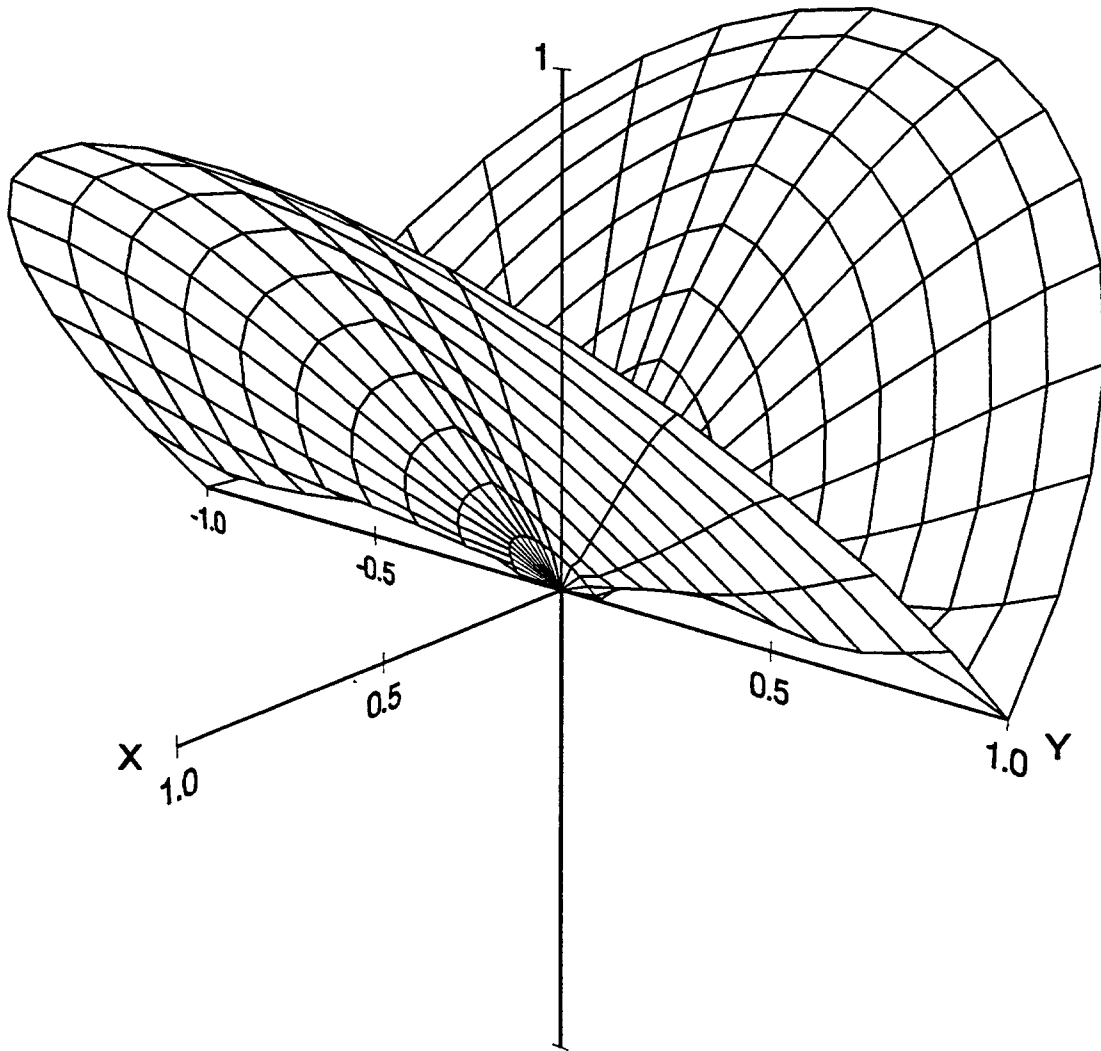
Dipole Diameter. In the present example the diameter of the electric dipole is taken as one-tenth the inner diameter of the tube or 0.22cm. Reducing the dipole thickness by a

Figure 3  
Relative Ez-field within a 2.2cm metal tube at Z = 1.1cm



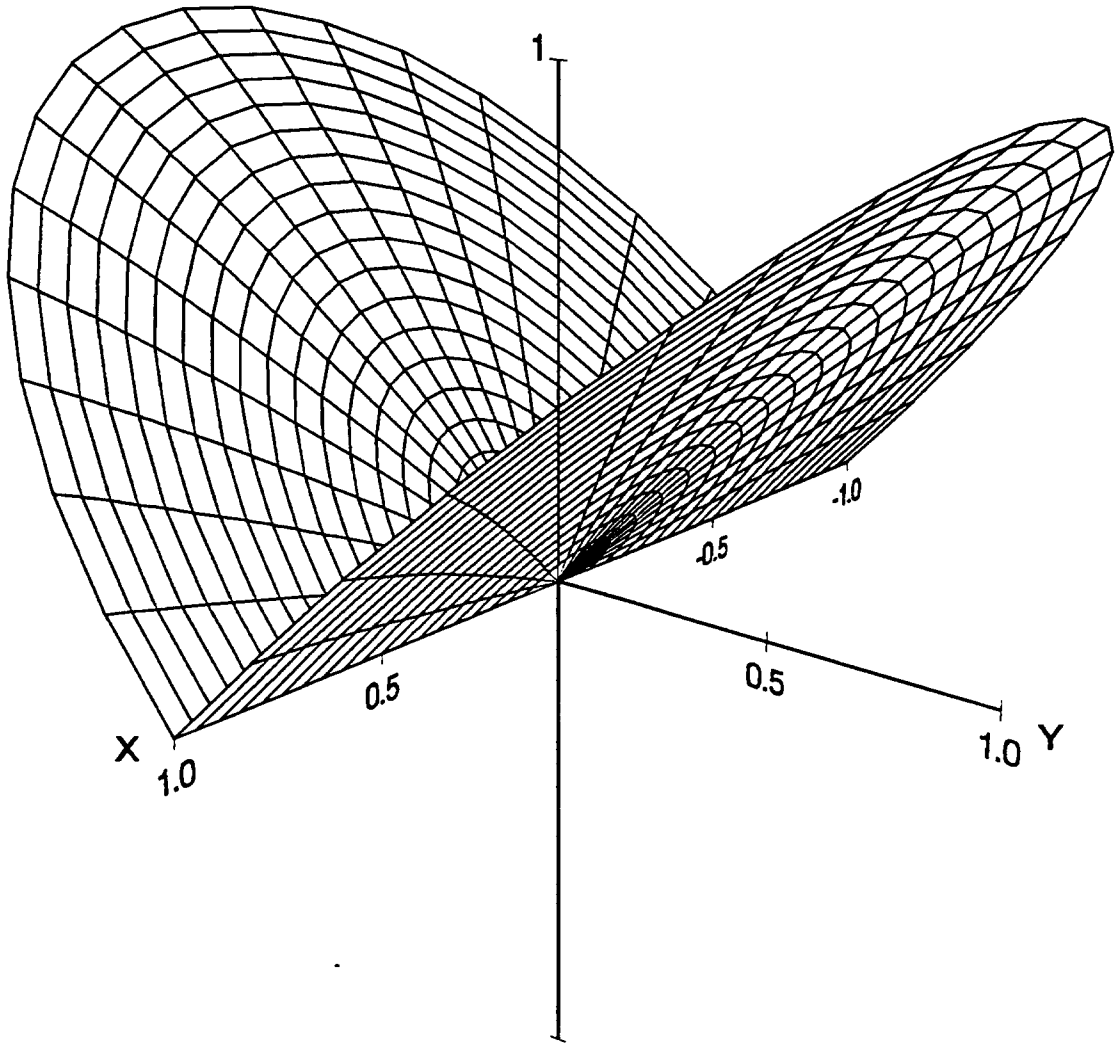
ctube8a.dcf  
ctube8a.dat  
ctube8a.wk1  
ctubeo.08a

Figure 4  
Relative Ez-field with a 2.2cm metal tube at Z = 2.2cm



ctube7a.dcf  
ctube7a.dat  
ctube7a.wk1  
ctubeo.07a

Figure 5  
Relative Ez-field within a 2.2cm air tube at Z = 2.2cm



cpri1a.dcf  
cpri1a.dat  
cpri1a.wk1  
cprio.01a

factor of four with the use of printed circuit techniques, and coupling directly to an integrated preamplifier, would raise the SCR from -5.1dB to 6.9dB and make the crack detectable.

## Conclusion

Numerical computations of the fields show that the use of a printed-circuit receiving dipole and integrated amplifier could detect cracks whose scattering loss is not less than -40dB. It would be desirable to develop a catalog of practical cracks which are found in a variety of pipe sizes and conductivities. A three-dimensional model code (Newman and Alumbaugh, 1996a, 1996b) could be used as a means of estimating the scattering loss of each catalog entry. The design and development of an instrument could be undertaken if the modeling showed that practical cracks have scattering losses greater than -40dB.

## References

- G. A. Newman and D. L. Alumbaugh, 1996a, *Electromagnetic Modeling of Subsurface 3D Structures*, Proceedings of the 1996 IEEE International Geoscience and Remote Sensing Symposium, Vol. IV, pp 1941-1944, Lincoln, Nebraska, May 1996. IEEE # 96CH35875.
- G. A. Newman and D. L. Alumbaugh, 1996b, *Three-Dimensional Electromagnetic Modeling and Inversion on Massively Parallel Computers*, Sandia National Laboratories report SAND96-0582, March 1996. Available from the U.S. Department of Commerce, Clearing-house for Federal Scientific and Technical Information, Springfield, VA.
- James R. Wait and David A. Hill, 1977, "Electromagnetic Fields of a Dipole Source in a Circular Tunnel Containing a Surface Wave Line", *International Journal of Electronics*, 1977, Vol. 42, No. 4, pp 377-391.

# APPENDIX

## Electromagnetic Fields in a Cylindrical Void within a Complex Media

The solution for the electromagnetic fields within a borehole surrounded by a complex homogeneous medium was included by J. R. Wait and David A. Hill as part of an article devoted to another topic [Wait and Hill, 1977]. The theory is summarized below with the authors' notation in which time-harmonic fields are assumed in accordance with  $\exp(j\omega t)$ .

### Geometry

Figure A1 depicts the XY-plane intercepted by a circular cylinder of radius ' $a_o$ ' whose axis is coincident with the Z-axis. A magnetic dipole, with its moment parallel to the X-axis, is located at cylindrical coordinates  $(\rho_l, \phi_l, 0)$  where  $\rho_l < a_o$ , and the field point is at  $(\rho, \phi, z)$  with  $\rho \leq a_o$ . The cylinder is air-filled with permeability  $\mu_o$  and dielectric constant  $\epsilon_o$ , and the surrounding homogeneous media has conductivity  $\sigma_e$  with permeability  $\mu_e$  and dielectric constant  $\epsilon_e$ .

### $E_z$ Field

The  $E_z$  field is represented as a superposition of modes in terms of the Hertz potentials which supply the modal contributions:

$$E_z = \sum_{m=-\infty}^{+\infty} \int_{-\infty}^{+\infty} -v^2 \{A_m(\lambda)K_m(v\rho) + P_m(\lambda)I_m(v\rho)\} \exp[-jm(\phi - \phi_l)] \exp(-j\lambda z) d\lambda \quad (A1)$$

where  $I_m(v\rho)$  and  $K_m(v\rho)$  are modified Bessel functions,  $v^2 = \lambda^2 + \gamma_o^2$  and  $\gamma_o = j\omega/c$ . The functions  $A_m(\lambda)$  and  $B_m(\lambda)$  are the primary Hertz potentials determined by the strength and orientation of the magnetic dipole source, and the secondary potential  $P_m(\lambda)$  is related to  $A_m(\lambda)$  and  $B_m(\lambda)$  by the boundary conditions at the cylinder/media interface.

### Hertz Potentials

When the X-directed magnetic dipole is located at  $Z = 0$ , the electric and magnetic Hertz potentials are given by these expressions when  $\rho_l < \rho$ :

$$A_m(\lambda) = \frac{-\mu_o \omega l dA}{8v\pi^2} [I_{m-1}(v\rho_l) \exp(-j\phi_l) - I_{m+1}(v\rho_l) \exp(j\phi_l)] \quad \text{V}\cdot\text{m}^2 \quad (A2)$$

and

$$B_m(\lambda) = \frac{-j\lambda l dA}{8v\pi^2} [I_{m-1}(v\rho_l) \exp(-j\phi_l) + I_{m+1}(v\rho_l) \exp(j\phi_l)] \quad \text{A}\cdot\text{m}^2 \quad (A3)$$

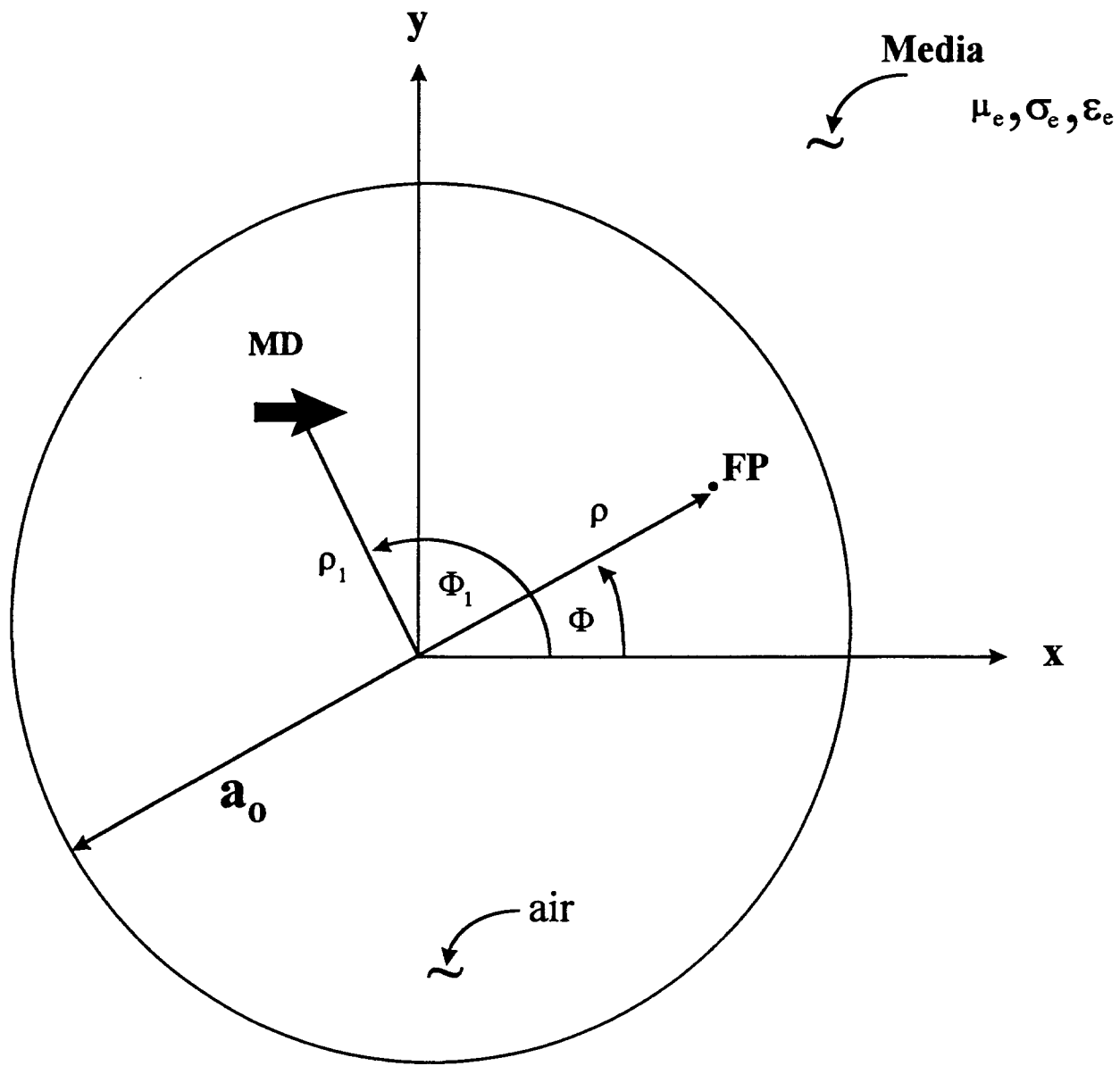


Figure A1  
 Cross-section geometry for a cylindrical void

### Boundary Conditions

The boundary conditions at the cylinder/media interface can be succinctly expressed in terms of a radial wave impedance  $Z_m$  and a radial wave admittance  $Y_m$  at  $\rho = a_o$  [Stratton, 1941]:

$$E_{\phi m} = \alpha_m E_{zm} + Z_m H_{zm} \quad (\text{A4})$$

$$H_{\phi m} = -Y_m E_{zm} + \alpha_m H_{zm} \quad (\text{A5})$$

where:

$$\alpha_m = m\lambda / (a_o u^2) \quad (\text{A6})$$

$$\gamma_e^2 = j\mu_e \omega (\sigma_e + j\omega \epsilon_e) \quad (\text{A7})$$

$$u^2 = \lambda^2 + \gamma_e^2 \quad (\text{A8})$$

$$Y_m = [j\gamma_e^2 / (u\mu_e \omega)] K'_m(u a_o) / K_m(u a_o) \quad (\text{A9})$$

$$Z_m = -(j\mu_e \omega / u) K'_m(u a_o) / K_m(u a_o) \quad (\text{A10})$$

The application of the boundary conditions establish the relation of the secondary potential,  $P_m$ , to the primary potentials  $A_m$  and  $B_m$ :

$$P_m = -[A_m(\lambda)r_m + B_m(\lambda)t_m] / D_m \quad \text{V}\cdot\text{m}^2 \quad (\text{A11})$$

where

$$r_m = \left[ \left( \frac{m\lambda}{a_o v^2} - \alpha_m \right)^2 + \left( \frac{\gamma_o K'_m}{v K_m} + \eta_o Y_m \right) \left( \frac{\gamma_o I'_m}{v I_m} + \frac{Z_m}{\eta_o} \right) \right] I_m K_m \quad (\text{A12})$$

$$t_m = \left( \frac{m\lambda}{a_o v^2} - \alpha_m \right) \frac{j\mu_o \omega}{a_o v^2} \quad (\text{A13})$$

$$D_m = \left[ \left( \frac{m\lambda}{a_o v^2} - \alpha_m \right)^2 + \left( \frac{\gamma_o I'_m}{v I_m} + \eta_o Y_m \right) \left( \frac{\gamma_o I'_m}{v I_m} + \frac{Z_m}{\eta_o} \right) \right] I_m^2 \quad (\text{A14})$$

and  $\eta_o = \sqrt{\mu_o \epsilon_o}$  is assumed to be the characteristic impedance of the air inside the cylinder. The argument of the modified Bessel functions is  $\alpha_o \nu$ , and the prime, ' , denotes differentiation with respect to  $\nu$ , the wavenumber within the cylinder.

### Computational Notes

In the special case where the magnetic dipole is located at the origin, the representations of the Hertz potentials are simplified and only two modes are needed, namely  $m = \pm 1$ . For example, Eq.(A2) for  $A_m(\lambda)$  becomes:

$$A_m = A^o [I_{m-1}(0) - I_{m+1}(0)] \quad (\text{A15})$$

with  $A^o = -\mu_o \omega I d A / (8 \nu \pi^2)$ . Using the properties of the Bessel functions (Abramowitz and Stegun, 1972),  $A_{-1} = A^o$ , and  $A_{+1} = -A^o$ , but  $A_m$  is zero for  $m = 0$ ,  $m \leq -2$ , and  $m \geq 2$ . Similarly,  $B_{-1} = B^o$ , and  $B_{+1} = -B^o$  where  $B^o$  is the leading factor, and all other  $B_m$  are zero.

As a check on both the code and the theory, it is of interest to see what happens when  $\gamma_e = \gamma_o$ , or when  $\alpha_o \rightarrow \infty$ . The secondary potential  $P_m$  becomes zero as required, and the field reduces to:

$$E_z = \sum_{m=\pm 1}^{+\infty} \int_{-\infty}^{+\infty} -\nu^2 \{A_m(\lambda) K_m(\nu \rho)\} \exp[-jm\phi] \exp[-j\lambda z] d\lambda \quad (\text{A16})$$

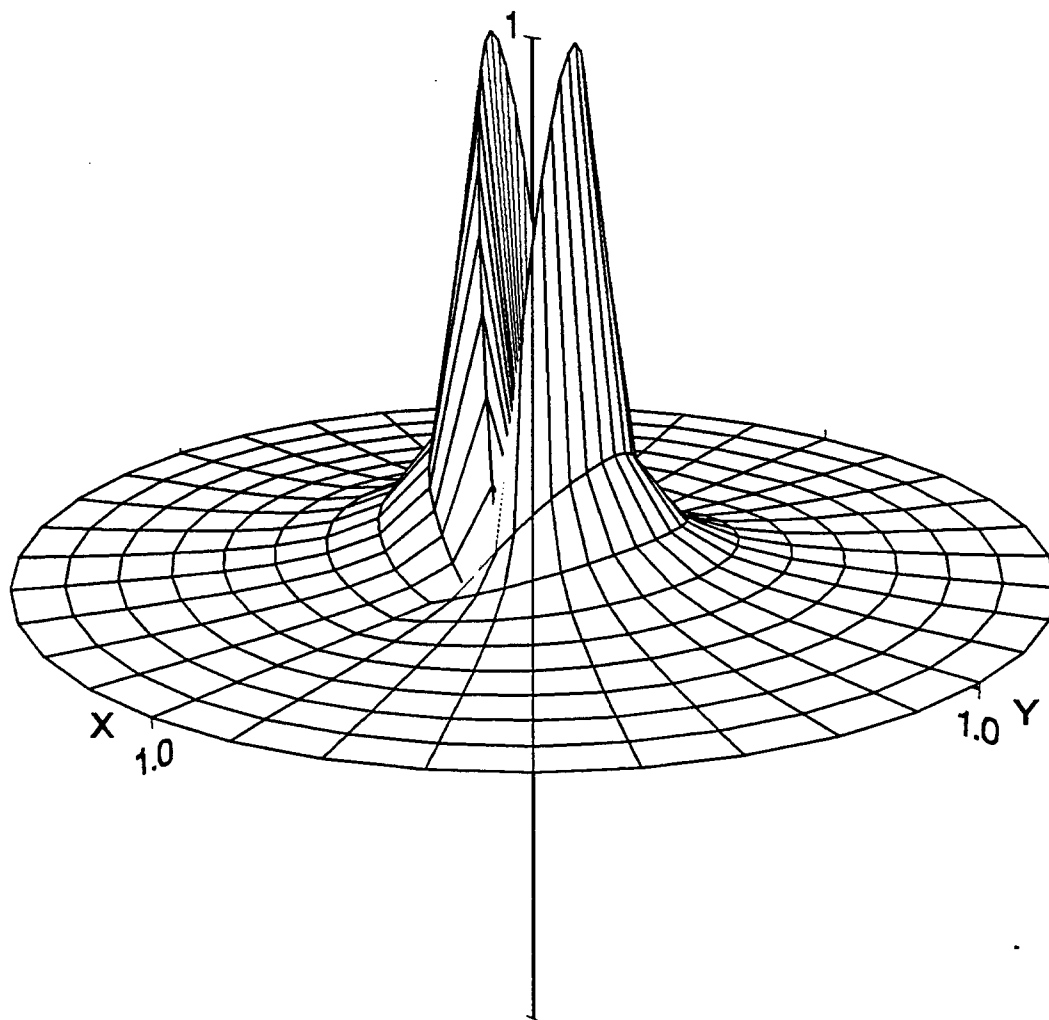
The closed-form solution for the dipole source in air is given by:

$$E_z = \frac{-j\mu_o \omega I d A}{4\pi} \sin \theta \sin \phi \left( \frac{jkR - 1}{R^2} \right) e^{jkR} \quad (\text{A17})$$

Eq.(A16) is undefined when  $\rho$  is zero, and Eq.(A17) is undefined when  $R$  is zero, because these respective radii would place the field-point at the location of the magnetic dipole.

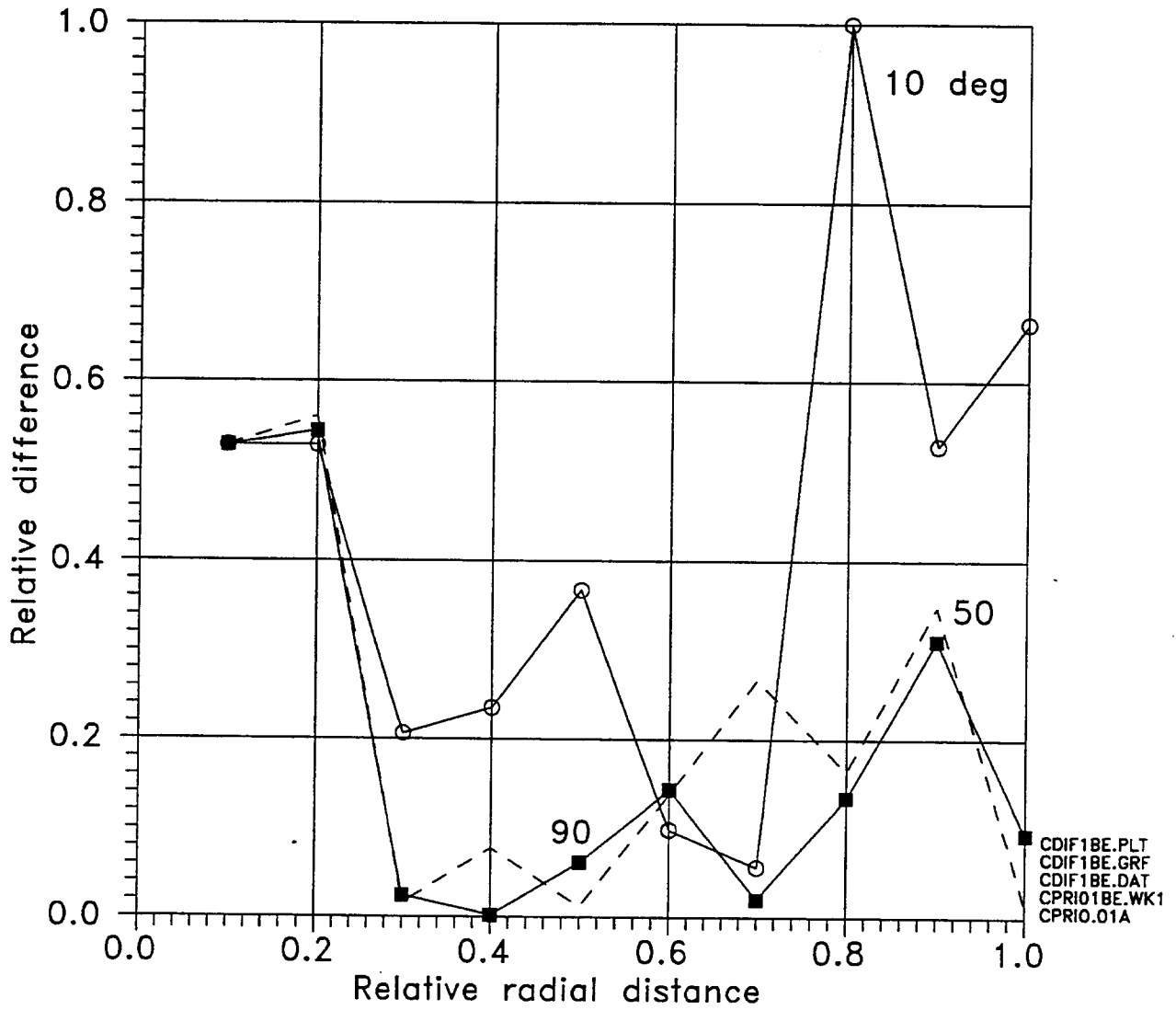
As a check, the magnitudes of these two formulas were compared for a frequency of 47.88KHz and  $\rho = 1.1\text{cm}$  in the  $XY$ -plane. The magnitude-plots overlap as shown in Figure A2 where the figure is dominated by double-peaks near the  $Z$ -axis. These occur because the field is computed ever more closely to the magnetic dipole located at the origin (where the graph is set to zero for display purposes). Along the rim of the figure, where the normalized radius is one, the magnitude varies as  $|\sin(\phi)|$  with maximums at  $90^\circ$  and  $180^\circ$  as required by Eq.(A17). The maximum difference between the two formulas is about 0.045% and is shown in Figure A3. This relative accuracy of less than one-percent is sufficient for practical purposes.

Figure A2  
Magnitude of the relative Ez-field in air  
within a radius of 1.1cm in the XY-plane



cpri01b.dcf  
cpri01b.dat  
cpri01b.wk1  
cprio.01a

Figure A3 Difference between computations with azimuth as a parameter. Max dif = 1/2075.



## References

- M. Abramowitz and I. A. Stegun, 1972, "*Handbook of Mathematical Functions*", Dover Publications Inc. New York, Sections 9.6.1-9.7.11.
- J. A. Stratton, 1941, "*Electromagnetic Theory*", McGraw-Hill, New York, pp 354-361, p532.
- James R. Wait and David A. Hill, 1977, "*Electromagnetic Fields of a Dipole Source in a Circular Tunnel Containing a Surface Wave Line*", International Journal of Electronics, 1977, Vol. 42, No. 4, pp 377-391.

## DISTRIBUTION:

- 1      Commissioner Kenneth C. Rogers  
U.S. Nuclear Regulatory Commission  
Washington, D. C. 20555-0001
  
- 1      National Institute of Science and Technology  
Attn: D. A. Hill, Mail Code 813.07  
325 Broadway  
Boulder, CO 80303
  
- 1      Raton Technology Research  
Attn: L. G. Stolarczyk  
P. O. Box 428  
Raton, NM 87740
  
- 1      MS 1072 F. W. Hewlett, Jr., 1273  
Attn: H. A. Watts
  
- 1      1134 B. J. Kelley, 1846
  
- 1      0188 C. E. Meyers, 4523
  
- 1      0701 R. W. Lynch, 6100
  
- 1      0705 L. C. Bartel, 6116
  
- 15     0705 T. W. H. Caffey, 6116
  
- 1      0750 D. L. Alumbaugh, 6116
  
- 1      0750 G. A. Newman, 6116
  
- 1      0750 M. C. Walck, 6116
  
- 1      0744 D. A. Powers, 6404
  
- 1      0741 J. M. Clauss, 6471
  
- 1      0741 J. T. Nakos, 6471
  
- 1      0747 A. L. Camp, 6412
  
- 1      0865 M. E. Morris, 9753
  
- 1      9018 Central Technical Files, 8940-2
  
- 5      0899 Technical Library, 4414
  
- 2      0619 Review & Approval Desk, 12690  
For DOE/OSTI

